Eur. Phys. J. D **15**, 267–277 (2001)

THE EUROPEAN PHYSICAL JOURNAL D

EDP Sciences

Resonance fluorescence spectrum of a three-level atom driven by coherent and stochastic fields

G. Li[1a], S. Wu[1], and P. Zhou[2]

[1] Department of Physics, Huazhong Normal University, Wuhan 430079, P.R. China
[2] School of Physics, Georgia Institute of Technology, Atlanta GA30332-0430, USA

Received 23 June 2000 and Received in final form 18 January 2001

Abstract. The dressed-state populations and the resonance fluorescence spectrum of a V-type three-level atom driven by a strong coherent field and a weak stochastic one simultaneously are investigated. There can be significant population inversion due to the effect of the stochastic field. The atomic resonance fluorescence spectrum can be controlled by adjusting the frequency difference between the coherent field and the stochastic one and the coherent Rabi frequency. Peak suppression and line narrowing occur under appropriate conditions.

PACS. 42.50.Hz Strong-field excitation of optical transitions in quantum systems; multi-photon processes; dynamic Stark shift – 42.50.Lc Quantum fluctuations, quantum noise, and quantum jumps

1 Introduction

It is well-known that when a two-level atom is driven by a strong coherent field, the resonance fluorescence spectrum exhibits a Mollow symmetric triplet [1], in which the locations of two sidebands depend on the generalized Rabi frequency and the relative heights and widths of the triplet are independent of the intensity of the laser field. Recently, considerable attention has been paid to modifying the standard resonance fluorescence spectrum. One way is to place the coherently driven atom inside a cavity, for which spectral features can be changed dramatically, for example, dynamical suppression and enhancement and spectral line narrowing of the Mollow triplet have been predicted [2,3] theoretically and observed [4,5] experimentally. Another method is to bathe the atom in a squeezed vacuum. It has been found [6,7] that the linewidths of the spectral characters strongly depend on the relative phase between the squeezed vacuum and the driving field, and can be broadened or narrowed compared to that in the ordinary vacuum. By use of the quantum interference induced by spontaneous emission for a multi-level system, the phenomena such as resonance fluorescence quenching and line narrowing have been revealed [8,9].

However, in the view of practice, a driving field may have amplitude or frequency fluctuations (or both), a lot of studies have been pursued on atomic response to fluctuating fields [10] and the modification of the Mollow triplet due to field fluctuations has been elucidated [11–13]. For an atom driven by a finite bandwidth laser, spectral broadening, sideband suppression, and asymmetry of the Mollow spectrum were predicted [11]. Recently, it has been shown [12,13] that in the system of a two-level atom driven by a strong coherent field as well as a weak stochastic field with wide bandwidth, the stochastic field may give rise to dramatic narrowing of the linewidths of all three peaks [12] and the appearance of a similar phase-sensitive spectral profiles in resonance fluorescence to that which occurs in the squeezed vacuum [13].

On the other hand, after the initial ideas [14] and experimental demonstration [15,16] of the feasibility of the control of photoabsorption and photoemission and their products through the control of the relative phase of two coherent fields (which was often termed as coherent control) much work in atoms [17] and molecules [16] has explored a variety of processes. Many interesting results have been revealed, establishing thus the idea as a useful tool. The effect of the relative phase of two coherent driving fields on the transient dynamics of two-level atoms has been investigated experimently [18], the measured fluorescence intensity is strongly phase-dependent. Schemes have also been proposed using the phase difference to control the quantum interference between different transition channels to manipulate spontaneous emission [19] and the shape of the Autler-Townes doublet [20] in multilevel atomic systems. However, the effects of the amplitude or frequency fluctuations (or both) are not taken into account. Different from the above coherent control method to manipulate the radiation properties of atoms, here we will stress that adjusting the central frequency

[a] e-mail: gaox@phys.ccnu.edu.cn

of a stochastic field with finite bandwidth can be used to modify the radiation properties significantly.

In this paper, we investigate the resonance fluorescence of a V-type three-level atom driven by a strong coherent field as well as a weak stochastic field with a wide bandwidth. We demonstrate that the atomic populations in dressed state representation, and fluorescence spectrum can be strongly controlled by adjusting the central frequency of the stochastic field. In Section 2, the model is described and an effective master equation for the reduced density operator of the atom is derived when the coherent driving field is much stronger than the stochastic field. For simplicity, we restrict our attention to the situation where the frequency of the coherent field is tuned to the mean Bohr frequency of the excited states. Section 3 is devoted to discussing the atomic population distribution in the dressed state representation. It is found that the populations in the dressed states are strongly dependent on the frequency detuning δ between the coherent field and the stochastic one. Under certain conditions, the populations may be inverted. The plots of the dressed states populations against δ are used to provide a understanding of the phenomena in the subsequent section. In Section 4, we study the effect of the stochastic field on the resonance fluorescence spectrum of the atom. Asymmetrically spectral features and spectral line narrowing can be reached by adjusting δ and Rabi frequency. These phenomena are owing to the dynamical control of the dressed state populations and the atomic transition rates. Finally we give a summary.

2 Model and master equation

Consider a V-configuration three-level atom consisting of two excited states $|1\rangle$ and $|2\rangle$ coupled to a common ground state $|0\rangle$, bichromatically driven by a coherent field with frequency $\omega_{\rm L}$ and a constant amplitude $E_{\rm c}$ as well as by a stochastic field with a center frequency $\omega_{\rm s}$ and a complex, stochastically fluctuating amplitude $E_{\rm s}(t)$. In the frame of the rotating wave approximation at the frequency $\omega_{\rm L}$, the master equation of the density matrix ρ for the system is of the form

$$\dot{\rho} = -\mathrm{i}[H_{\rm a-c} + H_{\rm a-s}, \rho] + \mathcal{L}_{\mathcal{A}}\rho, \tag{1}$$

where

$$H_{\rm a-c} = -(\omega_{21} - \Delta)A_{11} + \Delta A_{22} + \Omega_2(A_{02} + A_{20}) + \Omega_1(A_{01} + A_{10}), \tag{2}$$

$$H_{\rm a-s} = \frac{1}{2}\{\mathrm{e}^{-\mathrm{i}\delta t}[\chi_1(t)A_{10} + \chi_2(t)A_{20}] + \mathrm{e}^{\mathrm{i}\delta t}[\chi_1^* A_{01} + \chi_2^* A_{02}]\}, \tag{3}$$

$$\mathcal{L}_A\rho = \frac{\gamma_1}{2}(2A_{01}\rho A_{10} - \rho A_{11} - A_{11}\rho) + \frac{\gamma_2}{2}(2A_{02}\rho A_{20} - \rho A_{22} - A_{22}\rho). \tag{4}$$

Here $\mathcal{L}_A\rho$ characterizes the atomic damping due to the interaction of the vacuum field, γ_1 and γ_2 are the decay constants of the levels $|1\rangle$ and $|2\rangle$. $H_{\rm a-c}$ and $H_{\rm a-s}$ describe the interaction of the atom with the coherent field and stochastic field respectively, $\omega_{21} = \omega_2 - \omega_1$ is the level spacing of the two excited levels, $\Delta = \omega_2 - \omega_{\rm L}$ denotes the detuning between the frequency ω_2 of the atomic transition $|0\rangle \to |2\rangle$ and the frequency $\omega_{\rm L}$ of the coherent part of the driving field, $\delta = \omega_{\rm s} - \omega_{\rm L}$ is the frequency difference between the coherent and chaotic parts of the driving field, $2\Omega_i = 2|\mathbf{d}_{i0} \cdot \mathbf{e}E_{\rm c}|/\hbar$ $(i = 1, 2)$ is the Rabi frequency of the atomic transitions $|0\rangle \leftrightarrow |i\rangle$ $(i = 1, 2)$ under the interaction of the coherent component of the driving field, and $\chi_i(t) = 2\mathbf{d}_{i0} \cdot \mathbf{e}E_{\rm s}(t)/\hbar$ represents the amplitude of the stochastic field-atom interaction, which is assumed to be a complex Gaussian-Markovian random process with zero mean value and correlation functions

$$\langle \chi_i(t)\chi_j^*(t')\rangle = D_{ij}\kappa\mathrm{e}^{-\kappa|t-t'|}; \quad \langle \chi_i(t)\chi_j(t')\rangle = 0, \tag{5}$$

where D_{ij} is proportional to the strength of the stochastic process and κ can be associated with the bandwidth of the stochastic field. These correlation functions (Eq. (5)) describe a field undergoing both phase and amplitude fluctuations, which result in a finite bandwidth κ of the field. In the limit of $\kappa \to \infty$, the correlation reduces to a δ-function and the stochastic field is then a complex white noise field. For simplicity of calculation, we assume that $\Delta = \omega_{21}/2$ and $|\mathbf{d}_{10}| = |\mathbf{d}_{20}|$ so that $\gamma_1 = \gamma_2 = \gamma$, $\Omega_1 = \Omega_2 = \Omega$, $D_{ij} = D$.

Here we assume that the intensity of the coherent field is much greater than that of the stochastic field and the bandwidth κ of the stochastic field is much greater than the atomic linewidth (that is to say, the correlation time κ^{-1} of the stochastic field is very short compared to the radiative lifetime γ^{-1} of the atom), *i.e.*, $4\Omega^2 \gg D\kappa$, and $\kappa \gg \gamma$. In this limit one can invoke standard perturbative techniques to eliminate the stochastic variables $\chi_i(t)$ $(i, j = 1, 2)$ [5,12]. Consequently, the master equation for the reduced density operator ρ for the atom can be expressed as

$$\dot{\rho} = -\mathrm{i}[H_{\rm a-c}, \rho] - \frac{1}{4}([A_{01} + A_{02}, [S_+, \rho]] + [A_{10} + A_{20}, [S_-, \rho]]) + \mathcal{L}_A\rho, \tag{6}$$

where

$$S_- = D\kappa\int_0^\infty \mathrm{d}\tau\, \mathrm{e}^{-(\kappa+\mathrm{i}\delta)\tau}\mathrm{e}^{-\mathrm{i}H_{\rm a-c}\tau}(A_{01} + A_{02})\mathrm{e}^{\mathrm{i}H_{\rm a-c}\tau}$$
$$= B_0A_{00} + B_1A_{11} + B_2A_{22} + B_3A_{02} + B_4A_{20} + B_5A_{01} + B_6A_{10} + B_7A_{21} + B_8A_{12} = (S_+)^\dagger, \tag{7}$$

$$\begin{bmatrix} B_0 \\ B_1 \\ B_2 \\ B_3 \\ B_4 \\ B_5 \\ B_6 \\ B_7 \\ B_8 \end{bmatrix} = \begin{bmatrix} 8\eta^3 & 2\eta\epsilon^2 & 0 & -2\eta\epsilon^2 & -8\eta^3 \\ -\eta(1-\epsilon^2)/2 & \eta\epsilon(1-\epsilon) & -2\eta\epsilon & \eta\epsilon(1+\epsilon) & \eta(1-\epsilon^2)/2 \\ -\eta(1-\epsilon^2)/2 & -\eta\epsilon(1+\epsilon) & 2\eta\epsilon & -\eta\epsilon(1-\epsilon) & \eta(1-\epsilon^2)/2 \\ 2\eta^2(1+\epsilon) & \epsilon^2(1+\epsilon)/2 & 4\eta^2 & \epsilon^2(1-\epsilon)/2 & 2\eta^2(1-\epsilon) \\ -2\eta^2(1-\epsilon) & -4\eta^2\epsilon & 4\eta^2 & 4\eta^2\epsilon & -2\eta^2(1+\epsilon) \\ 2\eta^2(1-\epsilon) & \epsilon^2(1-\epsilon)/2 & 4\eta^2 & \epsilon^2(1+\epsilon)/2 & 2\eta^2(1+\epsilon) \\ 2\eta^2(1+\epsilon) & 4\eta^2\epsilon & 4\eta^2 & -4\eta^2\epsilon & -2\eta^2(1-\epsilon) \\ -\eta(1-\epsilon)^2/2 & -\eta\epsilon(1-\epsilon) & 0 & -\eta\epsilon(1+\epsilon) & \eta(1+\epsilon)^2/2 \\ -\eta(1+\epsilon)^2/2 & \eta\epsilon(1+\epsilon) & 0 & \eta\epsilon(1-\epsilon) & -\eta(1+\epsilon)^2/2 \end{bmatrix} \begin{bmatrix} f(-2) \\ f(-1) \\ f(0) \\ f(1) \\ f(2) \end{bmatrix} \tag{8}$$

with the coefficients B_i $(i = 0, 1, ...8)$ given by

see equation (8) above

with

$$\begin{aligned} f(n) &= \frac{D\kappa}{\kappa + \mathrm{i}(\delta + n\Omega_\mathrm{r})} \\ &= \mathcal{R}(n\Omega_\mathrm{r}) - \mathrm{i}\mathcal{I}(n\Omega_\mathrm{r}) \quad (n = 0, \pm 1, \pm 2), \\ \eta &= \frac{\Omega}{2\Omega_\mathrm{r}}, \quad \epsilon = \frac{\omega_{21}}{2\Omega_\mathrm{r}}, \end{aligned} \tag{9}$$

and $\Omega_\mathrm{r} = \sqrt{\omega_{21}^2 + 8\Omega^2}/2$ is a generalized Rabi frequency. The first term on the right-hand-side of equation (6) describes the coherent interaction between the atom and the coherent part of the driving field, while the second term represents the effect of the stochastic part of the driving field. The last term characterizes the spontaneous decay of the atom induced by the standard vacuum field.

From the modified master equation (6), one can obtain the equations of motion of the reduced density matrix elements for the atomic variables to be of the form

$$\begin{aligned} \dot{\rho}_{10} = &-\left[\frac{\gamma}{2} + \mathrm{i}(\Delta - \omega_{21}) + \frac{1}{4}(2B_5 + B_3)\right]\rho_{10} - \frac{B_3}{4}\rho_{20} \\ &+ \left[\mathrm{i}\Omega + \frac{1}{4}(B_1 - B_2 - B_7)\right]\rho_{12} \\ &+ \left(2\mathrm{i}\Omega - \frac{B_8}{4}\right)\rho_{11} + \left(\mathrm{i}\Omega + \frac{B_8}{4}\right)\rho_{22} + \frac{B_6}{2}\rho_{01} \\ &+ \frac{1}{4}(B_4 + B_6)\rho_{02} + \frac{1}{4}B_8\rho_{21} - \mathrm{i}\Omega \end{aligned} \tag{10}$$

$$\begin{aligned} \dot{\rho}_{20} = &-\left[\frac{\gamma}{2} + \mathrm{i}\Delta + \frac{1}{4}(2B_3 + B_5)\right]\rho_{20} - \frac{B_5}{4}\rho_{10} \\ &+ \left[\mathrm{i}\Omega + \frac{1}{4}(B_2 - B_1 - B_8)\right]\rho_{21} \\ &+ \left(2\mathrm{i}\Omega - \frac{B_7}{4}\right)\rho_{22} + \left(\mathrm{i}\Omega + \frac{B_7}{4}\right)\rho_{11} + \frac{B_4}{2}\rho_{02} \\ &+ \frac{1}{4}(B_4 + B_6)\rho_{01} + \frac{1}{4}B_7\rho_{12} - \mathrm{i}\Omega \end{aligned} \tag{11}$$

$$\begin{aligned} \dot{\rho}_{21} = &-\left[\gamma + \mathrm{i}\omega_{21} + \frac{1}{4}(B_3 + B_5^*)\right]\rho_{21} - \frac{B_5}{4}(\rho_{11} - \rho_{00}) \\ &- \frac{B_3^*}{4}(\rho_{22} - \rho_{00})\left[\mathrm{i}\Omega + \frac{1}{4}(B_2^* - B_0^*)\right]\rho_{20} \\ &+ \left[-\mathrm{i}\Omega + \frac{1}{4}(B_1 - B_0)\right]\rho_{01} + \frac{B_8^*}{4}\rho_{10} + \frac{B_7}{2}\rho_{02} \end{aligned} \tag{12}$$

$$\begin{aligned} \dot{\rho}_{11} = &-\left[\gamma + \frac{1}{4}(B_5 + B_5^*)\right]\rho_{11} + \frac{1}{4}(B_5 + B_5^*)\rho_{00} \\ &+ \left[\mathrm{i}\Omega + \frac{1}{4}(B_1^* - B_0^*)\right]\rho_{10} + \frac{B_7^*}{4}\rho_{20} + \frac{B_7}{4}\rho_{02} \\ &+ \left[-\mathrm{i}\Omega + \frac{1}{4}(B_1 - B_0)\right]\rho_{01} - \frac{B_3^*}{4}\rho_{12} - \frac{B_3}{4}\rho_{21} \end{aligned} \tag{13}$$

$$\begin{aligned} \dot{\rho}_{22} = &-\left[\gamma + \frac{1}{4}(B_3 + B_3^*)\right]\rho_{22} + \frac{1}{4}(B_3 + B_3^*)\rho_{00} \\ &+ \left[\mathrm{i}\Omega + \frac{1}{4}(B_2^* - B_0^*)\right]\rho_{20} + \frac{B_8^*}{4}\rho_{10} + \frac{B_8}{4}\rho_{01} \\ &+ \left[-\mathrm{i}\Omega + \frac{1}{4}(B_2 - B_0)\right]\rho_{02} - \frac{B_5}{4}\rho_{12} - \frac{B_5^*}{4}\rho_{21}. \end{aligned} \tag{14}$$

Equations (10–14) show that the effect of the stochastic field on the atom gives rise to incoherent damping terms, incoherent pumping terms, and quantum interference terms originating from incoherent damping and pumping processes. If the bandwidth κ of the stochastic field tends to infinity, *i.e.*, $\kappa \to \infty$, which means that the stochastic field is just a complex white noise field, then from equation (8) we see that B_i $(i = 0, 1, ..., 8)$ can be approximated as $B_3 = B_5 = D$ and $B_j = 0$ $(j \neq 3, 5)$. In this case, except the incoherent damping and pumping terms, there appear quantum interference terms in equations (10–14) (for example, $B_5\rho_{12}/4$ and $B_5^*\rho_{21}/4$ in Eq. (14)), these terms are very similar to the quantum interference terms arising from spontaneous emission when the two dipole moments of the V-type three-level atom are non-orthogonal [21]. Fleischhauer *et al.* [22] predicted that in a double Λ system, this quantum interference, originating from the incoherent pumping processes, can lead

to lasing without inversion and to an enhancement of refraction without absorption. Here, we consider the case of the bandwidth κ of the stochastic field being finite, so $B_i \neq 0$ $(i = 0, 1, ..., 8)$, then there appear a lot of extra quantum coherence terms related to B_i. All these quantum coherence terms, which reflecting the quantum interference due to incoherent pumping and damping processes, modify the atomic behavior such as atomic populations and resonance fluorescence spectrum significantly.

3 Steady-state populations in dressed state representation

In this section we focus our attention on the effect of the stochastic field on the steady-state behavior of the atomic populations in the dressed state representation. The dressed states, defined by the eigenvalue equation, $H_{\mathrm{a-c}}|\alpha\rangle = \lambda_\alpha|\alpha\rangle$, are of the form

$$\begin{aligned}
|a\rangle &= \frac{1}{2}[-(1-\epsilon)|2\rangle - (1+\epsilon)|1\rangle + 4\eta|0\rangle], \\
|b\rangle &= -2\eta|2\rangle + 2\eta|1\rangle + \epsilon|0\rangle], \\
|c\rangle &= \frac{1}{2}[(1+\epsilon)|2\rangle + (1-\epsilon)|1\rangle + 4\eta|0\rangle],
\end{aligned} \tag{15}$$

and the corresponding eigenvalues are $\lambda_a = -\Omega_{\mathrm{r}}$, $\lambda_b = 0$, and $\lambda_c = \Omega_{\mathrm{r}}$.

In the high field intensity limit, where the generalized Rabi frequency Ω_{r} is much larger than all relaxation rates, *i.e.*, $\Omega_{\mathrm{r}} \gg D, \gamma$, the coupling between atomic density matrix elements $\rho_{\alpha\beta}$ $(\alpha, \beta = a, b, c)$ associated with various frequencies may be omitted. Under the secular approximation, from equation (6) we can easily obtain the equations of motion for the populations in the dressed states in the following rate equation form

$$\begin{aligned}
\dot{\rho}_{aa} &= -(R_{ab} + R_{ac})\rho_{aa} + R_{ca}\rho_{cc} + R_{ba}\rho_{bb}, \\
\dot{\rho}_{bb} &= -(R_{bc} + R_{ba})\rho_{bb} + R_{cb}\rho_{cc} + R_{ab}\rho_{aa}, \\
\dot{\rho}_{cc} &= -(R_{ca} + R_{cb})\rho_{cc} + R_{ac}\rho_{aa} + R_{bc}\rho_{bb},
\end{aligned} \tag{16}$$

where $R_{\alpha\beta}$ $(\alpha, \beta = a, b, c)$ represent the atomic transition rates from one dressed state $|\alpha\rangle$ to another one $|\beta\rangle$, which are defined as follows

$$\begin{aligned}
R_{ca} &= R_{ac} = \frac{\gamma}{4}(1-\epsilon^4) + 2\eta^2[\mathcal{R}(2\Omega_{\mathrm{r}}) + \mathcal{R}(-2\Omega_{\mathrm{r}})], \\
R_{ba} &= \frac{\gamma}{2}(1-\epsilon^2)^2 + \frac{\epsilon^2}{2}\mathcal{R}(\Omega_{\mathrm{r}}), \\
R_{bc} &= \frac{\gamma}{2}(1-\epsilon^2)^2 + \frac{\epsilon^2}{2}\mathcal{R}(-\Omega_{\mathrm{r}}), \\
R_{ab} &= \frac{\gamma}{2}\epsilon^2(1+\epsilon^2) + \frac{\epsilon^2}{2}\mathcal{R}(\Omega_{\mathrm{r}}), \\
R_{cb} &= \frac{\gamma}{2}\epsilon^2(1+\epsilon^2) + \frac{\epsilon^2}{2}\mathcal{R}(-\Omega_{\mathrm{r}}).
\end{aligned} \tag{17}$$

The terms related to the spontaneous decay rate γ in the transition rates $R_{\alpha\beta}$ describe the spontaneous damping rate of the atom from the dressed state $|\alpha\rangle$ to $|\beta\rangle$. Evidently, due to the effect of the stochastic field, there appear extra terms associated with the Lorentz functions $\mathcal{R}(\pm\Omega_{\mathrm{r}})$ and $\mathcal{R}(\pm 2\Omega_{\mathrm{r}})$ in $R_{\alpha\beta}$. All the transition rates $R_{\alpha\beta}$ are strongly dependent on the frequency difference δ between the coherent field and the stochastic one. The Lorentz functions $\mathcal{R}(\pm\Omega_{\mathrm{r}})$ and $\mathcal{R}(\pm 2\Omega_{\mathrm{r}})$ introduce resonances at $\delta = \pm\Omega_{\mathrm{r}}$ and $\pm 2\Omega_{\mathrm{r}}$ into $R_{\alpha\beta}$. This resonance property reflects the fact that the coherent field-atom interaction forms a "dressed" atom whose energy-level structure is intensity dependent and whose spontaneous emission dominates at the five frequencies $\omega_{\mathrm{L}}, \omega_{\mathrm{L}} \pm \Omega_{\mathrm{r}}, \omega_{\mathrm{L}} \pm 2\Omega_{\mathrm{r}}$. The dressed atom is then driven by the stochastic field. Therefore, when the central frequency of the stochastic field is tuned to these frequencies, the corresponding atomic transition is enhanced. This resonance property of the transition rates may lead to the resonance structures at four points $\delta = \pm\Omega_{\mathrm{r}}, \pm 2\Omega_{\mathrm{r}}$ in the dressed-state populations ρ_{ii} $(i = a, b, c)$.

Equations (17) show that the transition rates R_{ca} and R_{ac} contain two Lorentz functions $\mathcal{R}(\pm 2\Omega_{\mathrm{r}})$. These two Lorentz functions in R_{ca} and R_{ac} originate from different physical processes. Because the impact of the stochastic field with wide bandwidth on the atom gives rise to incoherent pumping and incoherent damping simultaneously, the component $\mathcal{R}(-2\Omega_{\mathrm{r}})$ in the transition rate R_{ca} (R_{ac}) reflects the incoherent damping (pumping) from the dressed state $|c\rangle$ $(|a\rangle)$ to $|a\rangle$ $(|c\rangle)$, and the other one $\mathcal{R}(2\Omega_{\mathrm{r}})$ in R_{ca} (R_{ac}) characterizes the incoherent pumping (damping) from $|c\rangle$ $(|a\rangle)$ to $|a\rangle$ $(|c\rangle)$. But the other rates related to the middle dressed state $|b\rangle$ contain only one Lorentz function $\mathcal{R}(\Omega_{\mathrm{r}})$ or $\mathcal{R}(-\Omega_{\mathrm{r}})$. The term containing $\mathcal{R}(\Omega_{\mathrm{r}})$ $(\mathcal{R}(-\Omega_{\mathrm{r}}))$ in R_{ba} (R_{bc}) arises from the incoherent pumping processes from $|b\rangle$ to $|a\rangle$ $(|c\rangle)$, and the term associated with $\mathcal{R}(\pm\Omega_{\mathrm{r}})$ in R_{ab} and R_{cb} is responsible for the incoherent damping processes from $|a\rangle$ and $|c\rangle$ to $|b\rangle$, respectively. That is to say, both the incoherent damping and pumping rates appear in R_{ca} and R_{ac} due to the effect of the stochastic field, but only the damping or pumping rate in the transition rates is associated with the dressed state $|b\rangle$. This is because for the system considered here, a coherently driven V-type three-level atom interacting with a stochastic field, there exists nine double-channels for the atomic transition from the dressed states $|\alpha\rangle$ to $|\beta\rangle$, which originate from the atomic bare state transitions $|1\rangle \leftrightarrow |0\rangle$ and $|2\rangle \leftrightarrow |0\rangle$ respectively. Constructive or destructive interference happens within every double-channel. For the incoherent damping processes, the two double-channels for the transitions $|b\rangle \rightarrow |c\rangle$ and $|b\rangle \rightarrow |a\rangle$ are completely destructive for the stochastic field, that is, the transitions from $|b\rangle$ to $|c\rangle$ and $|b\rangle$ to $|a\rangle$ never result in the emission of a photon into the stochastic field. So no terms reflecting the incoherent damping processes due to the effect of the stochastic field appear in R_{ba} and R_{bc}. At the same time, the other seven double-channels are still open to the stochastic field, which leads to the appearance of the incoherent damping rates in R_{ca}, R_{ac}, R_{ab} and R_{cb}. However, for the incoherent pumping processes induced by the stochastic field, the two double-channels for the transitions $|c\rangle \rightarrow |b\rangle$ and $|a\rangle \rightarrow |b\rangle$ are completely destructive for the stochastic field, which means that the

$$\rho_{cc} = \frac{R_{bc}(R_{ac}+R_{ab}+R_{ba})+R_{ba}(R_{ac}-R_{bc})}{(R_{ac}+R_{ab}+R_{ba})(R_{ca}+R_{cb}+R_{bc})-(R_{ca}-R_{ba})(R_{ac}-R_{bc})},$$
$$\rho_{aa} = \frac{R_{ba}(R_{ca}+R_{cb}+R_{bc})+R_{bc}(R_{ca}-R_{ba})}{(R_{ac}+R_{ab}+R_{ba})(R_{ca}+R_{cb}+R_{bc})-(R_{ca}-R_{ba})(R_{ac}-R_{bc})},$$
$$\rho_{bb} = 1-\rho_{aa}-\rho_{cc}. \tag{18}$$

$$\rho_{cc}-\rho_{aa} = \frac{\gamma\epsilon^2(3\epsilon^2-1)[\mathcal{R}(-\Omega_{\rm r})-\mathcal{R}(\Omega_{\rm r})]/2}{(R_{ac}+R_{ab}+R_{ba})(R_{ca}+R_{cb}+R_{bc})-(R_{ca}-R_{ba})(R_{ac}-R_{bc})} \tag{19}$$

transitions from $|c\rangle$ to $|b\rangle$ and from $|a\rangle$ to $|b\rangle$ never result in the absorption of a photon in the stochastic field. Consequently, there is no term describing the incoherent pumping processes in R_{cb} and R_{ab}. Likewise, the other seven double-channels remain open to the absorption of photons in stochastic field, thus, there exist the terms related to the incoherent pumping rates in other transition rates. Therefore, the transition rates R_{ca} and R_{ac} consist of two Lorentz functions $\mathcal{R}(\pm 2\Omega_{\rm r})$, one is from incoherent pumping processes and the other one from the incoherent damping processes due to the effect of the stochastic field, but the other rates $R_{\alpha\beta}$ related to the dressed state $|b\rangle$ only contain one Lorentz function, which reflects the effect of the incoherent pumping processes or the effect of the incoherent damping processes separately.

The steady-state dressed populations are obtained from equations (16) to be

see equations (18) above.

The dressed state populations are plotted as a function of the detuning in Figure 1. These plots have been obtained by a numerical solution of equations (10–15), but we have found that equations (18) provide an excellent approximation in the high field intensity limit.

It is evident that if the excited levels of the V-configuration three-level atom are nearly degenerate ($\epsilon \approx 0$) as shown in Figure 1a, the populations in the dressed states are not sensitive to the frequency detuning δ and ρ_{bb} approaches to zero. This is because when $\epsilon^2 \approx 0$, the transitions $|a\rangle \to |b\rangle$ and $|c\rangle \to |b\rangle$ are turned off (as $R_{ab}, R_{cb} \propto \epsilon^2$), whereas the rate of the transitions out of $|b\rangle$ is nonzero, therefore there is no steady-state population in the middle dressed state $|b\rangle$, all the populations are accumulated in the upper and lower dressed states $|c\rangle$ and $|a\rangle$. In this case, equations (18) are approximated to be: $\rho_{bb} \approx 0$, $\rho_{cc} \approx \rho_{aa} \approx 1/2$. That is to say, the populations in the dressed states are not sensitive to δ. In general, in regime $8\Omega^2 \gg \omega_{21}^2$, the population in $|b\rangle$ would be very small and ρ_{ii} $(i = a, b, c)$ would be not sensitive to δ. In Figure 1e ($\Omega = 150$) and Figure 1f ($\Omega = 300$), where we are only beginning to approach this limit, the behavior is similar. As we see, in the neighborhood of $\delta = \pm 2\Omega_{\rm r}$, no resonant structures appear in ρ_{ii} and ρ_{bb} is very small, whilst the resonant structures remain only around $\delta = \pm\Omega_{\rm r}$.

If the level spacing of the two excited states is large and the Rabi frequency is not very high, as shown in Figures 1b and 1c, the populations ρ_{ii} exhibit resonant structures at $\delta = \pm\Omega_{\rm r}$ and $\pm 2\Omega_{\rm r}$. However, Figures 1b and 1c show that in the negative region of δ, $\rho_{aa} > \rho_{cc}$, and in the positive domain of δ, $\rho_{aa} < \rho_{cc}$. And in Figures 1e and 1f, this frequency-detuning-dependent property is reversed. As mentioned above, the transitions rates $\mathcal{R}(\alpha\beta)$ consist of the spontaneous damping rates, the incoherent damping rates and the incoherent pumping rates arising from the effect of the stochastic field. The competition between the damping and the pumping processes may lead to different frequency-detuning-dependent properties of $\rho_{cc} - \rho_{aa}$. From equation (19) the population difference between the dressed states $|c\rangle$ and $|a\rangle$ can be written as

see equation (19) above.

Evidently, if $\epsilon^2 > 1/3$, *i.e.*, $\omega_{21} > 2\Omega$, then in the negative region of δ, $\rho_{cc} < \rho_{aa}$ since $\mathcal{R}(-\Omega_{\rm r}) < \mathcal{R}(\Omega_{\rm r})$, whilst in the positive region of δ, $\rho_{aa} < \rho_{cc}$ as shown in Figures 1b and 1c. When $\epsilon^2 < 1/3$, *i.e.*, $\omega_{21} < 2\Omega$, $\rho_{cc} > \rho_{aa}$ for $\delta < 0$ and $\rho_{aa} > \rho_{cc}$ for $\delta > 0$ as shown in Figures 1e and 1f. In Frame 1d ($\Omega = 110$) we see that for $\delta < 0$, ρ_{aa} may be less or larger than ρ_{cc}. This is because when we derive equations (16), the secular approximation is used and the contribution of the nondiagonal matrix elements are neglected. However as we see, the approximated critical relation $\omega_{21} = 2\Omega$ is coincides with the numerical results very well. So due to the effects of the stochastic field, there exists a critical relation between the level spacing of two excited states and the Rabi frequency to lead to $\rho_{cc} > \rho_{aa}$ or $\rho_{cc} < \rho_{aa}$ for the same frequency detuning δ.

However, in the limit of the bandwidth $\kappa \to \infty$, *i.e.*, the correlation in equation (5) reduces to a δ-function and the stochastic field is a complex white noise field, $\mathcal{R}(-\Omega_{\rm r}) \approx \mathcal{R}(\Omega_{\rm r}) = D$ and equations (18) then becomes

$$\rho_{cc} = \rho_{aa} = \frac{\gamma(1-\epsilon^2)^2+\epsilon^2 D}{\gamma(3\epsilon^4-3\epsilon^2+2)+3\epsilon^2 D}\,.$$

That is to say, population inversion between the upper dressed state $|c\rangle$ and the lower one $|a\rangle$ can never happen, which is similar to the case in the absence of the stochastic field [8]. So the population inversion in the dressed-state representation should be attributed to the transition rates $R_{\alpha\beta}$ dependent on the frequency detuning δ when the bandwidth κ of the stochastic field is finite. In other words, equations (6–9) indicate that the stochastic field with finite bandwidth forms a frequency-dependent

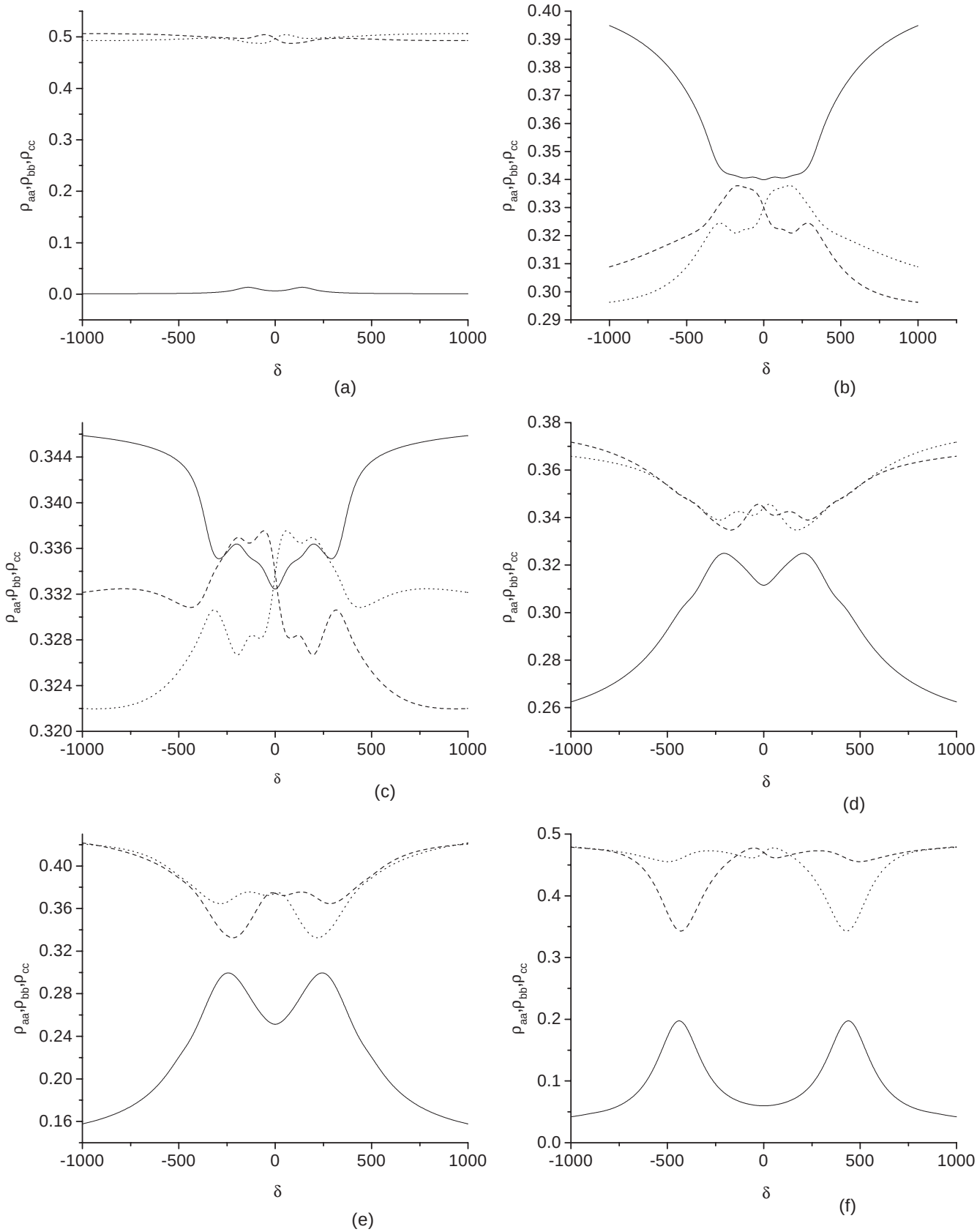

Fig. 1. The dressed-state populations against δ. ρ_{bb} is represented by a solid line, ρ_{aa} by a dashed line, and ρ_{cc} by a dotted line. In Frame (a) we take $\Omega = 100$ and $\omega_{21} = 10$, in Frames (b–f) we set $\omega_{21} = 200$ and $\Omega = 90, 98, 110, 150, 300$, respectively. The other parameters are taken to be: $\gamma = 1, D = 40, \kappa = 80$.

bath for the V-type three-level atom, tailoring this bath through adjusting the frequency detuning δ can be used to realize the population inversion.

4 Resonance fluorescence spectrum

The fluorescence emission spectrum is composed of coherent and incoherent components [16]. The coherent Raleigh part, whose origin can be traced to the elastic scattering of the coherent driving field, gives rise to only δ-function contributions, while the incoherent part stems from the fluctuations of the dipole polarizations. Hereafter we pay attention only to the incoherent resonance fluorescence spectrum, which is defined as

$$\Lambda(\omega) = \mathrm{Re}\int_0^\infty \mathrm{d}\tau\, \mathrm{e}^{-\mathrm{i}\omega\tau}\gamma[\langle \Delta A_{10}(t+\tau)\Delta A_{01}(t)\rangle + \langle \Delta A_{20}(t+\tau)\Delta A_{02}(t)\rangle]|_{t\to\infty} \quad (20)$$

where $\Delta A_{ij}(\tau) = A_{ij}(\tau) - \langle A_{ij}(\infty)\rangle$ represents the deviation of the atomic operator $A_{ij}(\tau)$ from its mean steady-state value. The two-time correlation functions $\lim_{t\to\infty}\langle \Delta A_{i0}(t+\tau)\Delta A_{0j}(t)\rangle$ can be obtained by use of the quantum regression theorem [23], together with the optical Bloch equations (10–14). To do this, we define vectors $\mathbf{R}_k(t)$ $(k = 1, 2)$ for the steady-state two-time correlations of the atom

$$\begin{aligned}\mathbf{R}_k(t) =[&\langle \Delta A_{20}(t)\Delta A_{0k}(0)\rangle,\ \langle \Delta A_{02}(t)\Delta A_{0k}(0)\rangle,\\ &\langle \Delta A_{22}(t)\Delta A_{0k}(0)\rangle,\ \langle \Delta A_{10}(t)\Delta A_{0k}(0)\rangle,\\ &\langle \Delta A_{01}(t)\Delta A_{0k}(0)\rangle,\ \langle \Delta A_{11}(t)\Delta A_{0k}(0)\rangle,\\ &\langle \Delta A_{21}(t)\Delta A_{0k}(0)\rangle,\ \langle \Delta A_{12}(t)\Delta A_{0k}(0)\rangle]^T. \quad (21)\end{aligned}$$

According to the quantum regression theorem, for $t > 0$ we have

$$\frac{\mathrm{d}}{\mathrm{d}t}\mathbf{R}_k(t) = M\mathbf{R}_k(t) \quad (k = 1, 2), \quad (22)$$

where M is a 8×8 matrix whose explicit expression can be easily derived from equations (10–14) by the definition of Bloch vector $[\langle A_{20}(t)\rangle, \langle A_{02}(t)\rangle, \langle A_{22}(t)\rangle, \langle A_{10}(t)\rangle, \langle A_{01}(t)\rangle, \langle A_{11}(t)\rangle, \langle A_{21}(t)\rangle, \langle A_{12}(t)\rangle]^T$. Taking the Fourier transformation of equation (20), in the long time limit, *i.e.*, $t \to \infty$, we find the incoherent fluorescence spectrum in the form

$$\Lambda(\omega) = \mathrm{Re}\sum_{j=1}^{8}\gamma[L_{1j}(\mathrm{i}\omega)R_2^{(j)}(0) + L_{4j}(\mathrm{i}\omega)R_1^{(j)}(0)], \quad (23)$$

where $R_k^{(j)}(0)$ is the initial component of the vector $\mathbf{R}_k(t)$ $(k = 1, 2)$, which defined in equation (19). $L_{kj}(\mathrm{i}\omega)$ is one element of the matrix $L(\mathrm{i}\omega) = (\mathrm{i}\omega I - M)^{-1}$, while I is the identity matrix.

Figures 2–4 exhibit the effects of the relative frequencies of the coherent and stochastic fields on the resonance

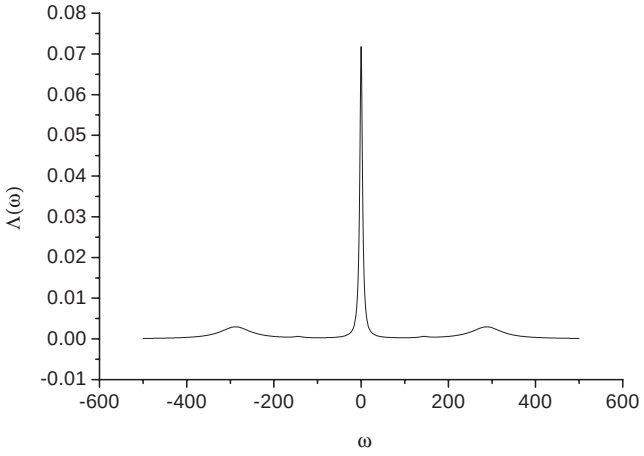

(a)

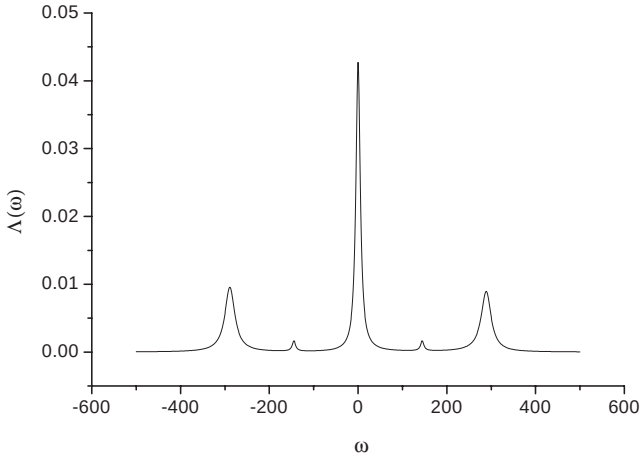

(b)

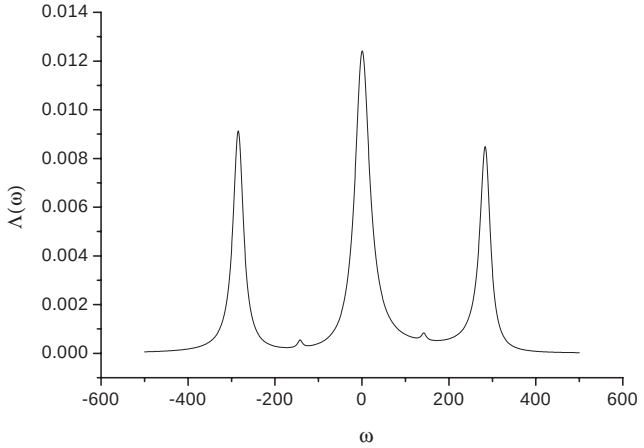

(c)

Fig. 2. The resonance fluorescence spectrum for $\kappa = 80$, $D = 40$ and $\gamma = 1$, $\omega_{21} = 10$, $\Omega = 100$, and (a) $\delta = 0$, (b) $\delta = \Omega_\mathrm{r}$, and (c) $\delta = 2\Omega_\mathrm{r}$.

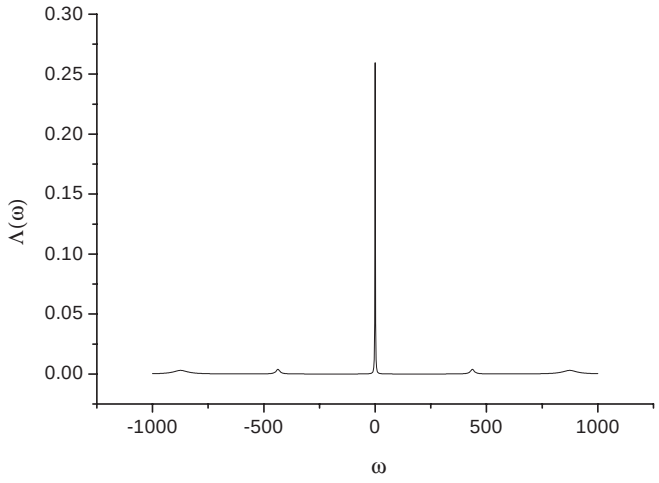

(a)

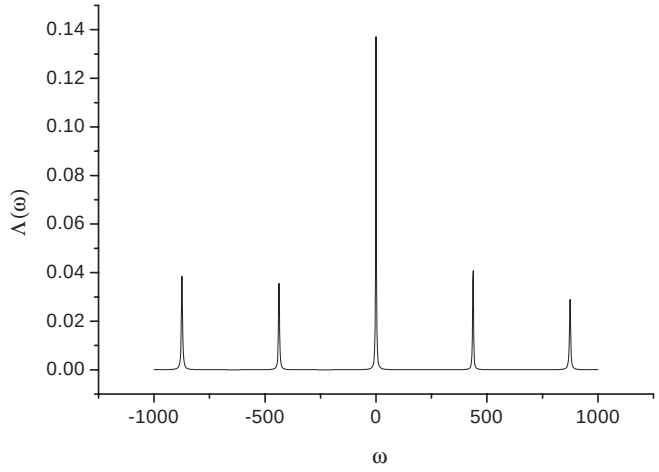

(b)

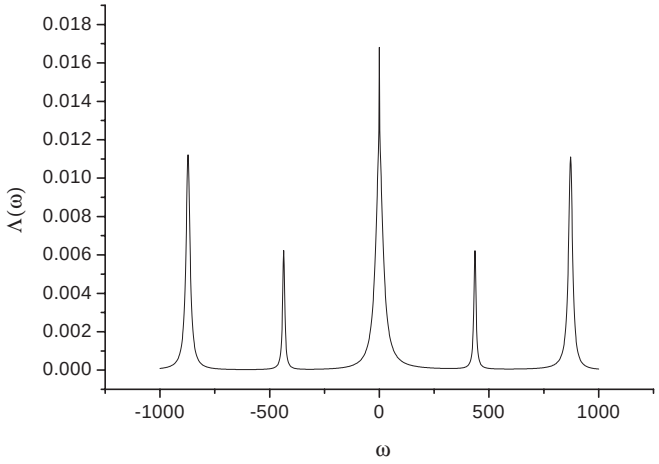

(c)

Fig. 3. Same as Figure 2 except $\omega_{21} = 200$ and $\Omega = 300$.

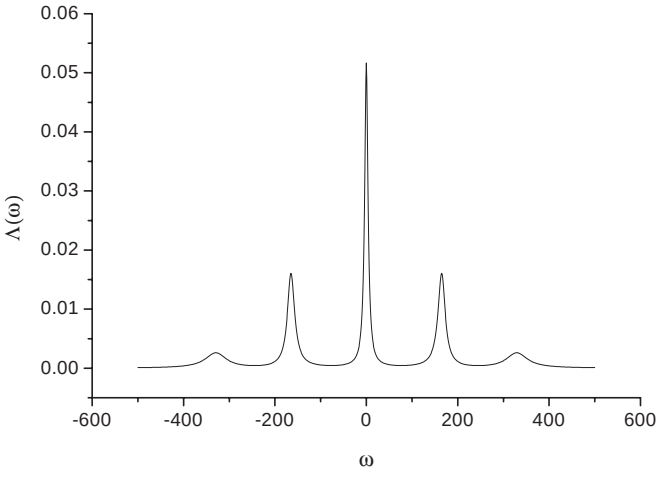

(a)

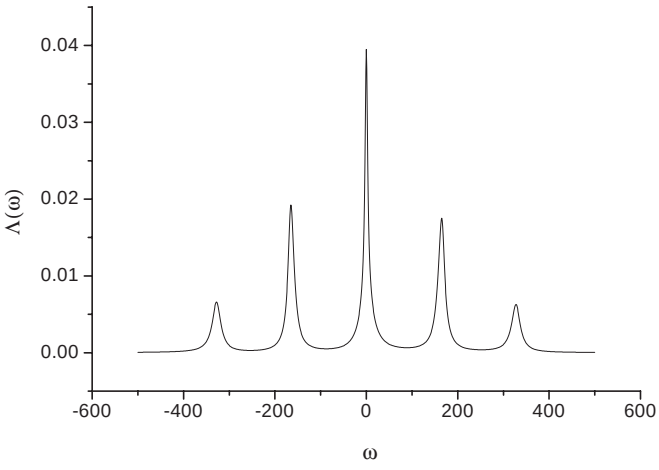

(b)

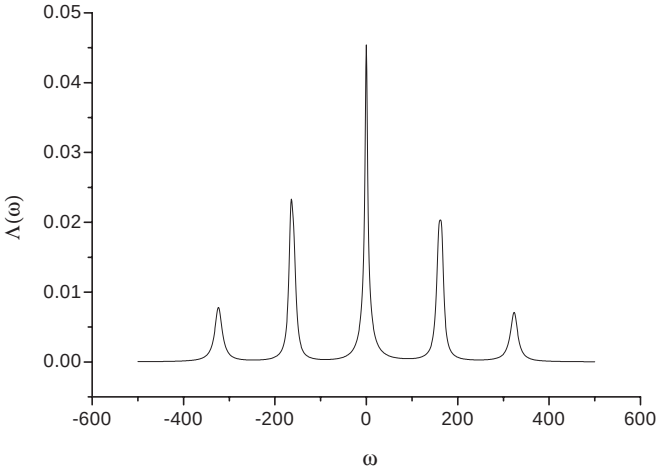

(c)

Fig. 4. Same as Figure 2 except $\omega_{21} = 200$ and $\Omega = 90$.

fluorescence spectrum. The spectra vary drastically with the frequency of the stochastic field. For example, if the central frequency of the stochastic field is the same as that of the coherent field, *i.e.*, $\delta = 0$, Figures 2a, 3a and 4a show that the fluorescence spectrum exhibits five symmetric peaks located at $\omega_{\rm L}, \omega_{\rm L} \pm \Omega_{\rm r}$ and $\omega_{\rm L} \pm 2\Omega_{\rm r}$. The central peak is much higher and narrower than the inner and outer sidebands. When the stochastic field is tuned to resonate with one of the sidebands, the spectrum becomes asymmetric and the central peak is suppressed and broadened while the sidebands are enhanced and narrowed as displayed in Figures 2b, 2c, 3b, 3c, 4b and 4c.

The physics associated with the spectral line narrowing and asymmetries arising from the effect of the stochastic field can be easily explored by working in the semiclassical dressed-state representation. In the high field intensity limit, where the effective Rabi frequency $\Omega_{\rm r}$ is much larger than all relaxation rates, *i.e.*, $\Omega_{\rm r} \gg \gamma, D$, the dressed energy levels are well separated, one can apply the secular approximation to simplify the equations of motion for the atomic density matrix elements in the dressed state representation, which are obtained according to equation (6) as

$$\begin{aligned}
\dot\rho_{aa} &= -\Gamma_{1+}\rho_{aa} + \Gamma_{2+}\rho_{cc} + R_{ba},\\
\dot\rho_{cc} &= -\Gamma_{1-}\rho_{cc} + \Gamma_{2-}\rho_{aa} + R_{bc},\\
\dot\rho_{ab} &= -(\Gamma_{3+} - {\rm i}\Omega_{3+})\rho_{ab} - \Gamma_4\rho_{bc},\\
\dot\rho_{bc} &= -(\Gamma_{3-} - {\rm i}\Omega_{3-})\rho_{bc} - \Gamma_4\rho_{ab},\\
\dot\rho_{ac} &= -(\Gamma_5 - {\rm i}\Omega_5)\rho_{ac}
\end{aligned} \tag{24}$$

where

$$\begin{aligned}
\Gamma_{1\pm} &= (\gamma/4)(3 - 2\epsilon^2 + 3\epsilon^4)\\
&\quad + 2\eta^2[\mathcal{R}(2\Omega_{\rm r}) + \mathcal{R}(-2\Omega_{\rm r})] + \epsilon^2\mathcal{R}(\pm\Omega_{\rm r}),\\
\Gamma_{2\pm} &= (\gamma/4)(1-\epsilon^2)(3\epsilon^2 - 1)\\
&\quad + 2\eta^2[\mathcal{R}(2\Omega_{\rm r}) + \mathcal{R}(-2\Omega_{\rm r})] - (\epsilon^2/2)\mathcal{R}(\pm\Omega_{\rm r}),\\
\Gamma_{3\pm} &= (\gamma/4)(3 + \epsilon^2 - 2\epsilon^4) + \eta^2[2\mathcal{R}(0) + \mathcal{R}(2\Omega_{\rm r})\\
&\quad + \mathcal{R}(-2\Omega_{\rm r})] + \epsilon^2[\mathcal{R}(\pm\Omega_{\rm r})/2 + \mathcal{R}(\mp\Omega_{\rm r})/4],\\
\Gamma_4 &= (\gamma/2)\epsilon^2(1-\epsilon^2),\\
\Gamma_5 &= (\gamma/4)(3+\epsilon^4) + 2\eta^2[4\mathcal{R}(0) + \mathcal{R}(2\Omega_{\rm r})\\
&\quad + \mathcal{R}(-2\Omega_{\rm r})] + (\epsilon^2/4)[\mathcal{R}(\Omega_{\rm r}) + \mathcal{R}(-\Omega_{\rm r})],\\
\Omega_{3\pm} &= \Omega_{\rm r} + \eta^2[\mathcal{I}(2\Omega_{\rm r}) - \mathcal{I}(-2\Omega_{\rm r})]\\
&\quad \pm \epsilon^2[\mathcal{I}(\pm\Omega_{\rm r})/2 + \mathcal{I}(\mp\Omega_{\rm r})/4],\\
\Omega_5 &= 2\Omega_{\rm r} + 2\eta^2[\mathcal{R}(2\Omega_{\rm r}) - \mathcal{R}(-2\Omega_{\rm r})]\\
&\quad + (\epsilon^2/4)[\mathcal{I}(\Omega_{\rm r}) - \mathcal{I}(-\Omega_{\rm r})],
\end{aligned} \tag{25}$$

where Γ_i is the decay rate in the dressed state representation, which is dependent on the frequency difference between the coherent and the stochastic parts of the driving field, when the central frequency of the stochastic field is tuned to $\delta = 0, \pm\Omega_{\rm r}$ and $\pm 2\Omega_{\rm r}$, the transition rates can be enlarged or reduced significantly. The parameters $\Omega_{\rm r} - \Omega_{3\pm}$ and $2\Omega_{\rm r} - \Omega_5$ represent the frequency shifts owing to the effect of the stochastic field. In the high field intensity limit, these shifts are negligibly small.

In the dressed state representation, the underlying physical processes are very transparent. For example, the downward transitions between the same dressed states of two adjacent dressed-state triplets give rise to the central component of the fluorescence spectrum, *i.e.*,

$$\Lambda_0(\omega) = {\rm Re}\left[2\eta^2 \frac{N_0(s)}{(s+\Gamma_{1+})(s+\Gamma_{1-}) - \Gamma_{2+}\Gamma_{2-}}\right]_{s={\rm i}\omega}, \tag{26}$$

with

$$\begin{aligned}
N_0(s) =& 2(2s + \Gamma_{1+} + \Gamma_{1-} - \Gamma_{2+} - \Gamma_{2-})\rho_{aa}\rho_{cc}\\
&- (1 - 9\epsilon^2)(\Gamma_{2+}\rho_{cc} + \Gamma_{2-}\rho_{aa})\rho_{bb}\\
&+ (1 + 9\epsilon^2)[(s+\Gamma_{1-})\rho_{aa} + (s+\Gamma_{1+})\rho_{cc}]\rho_{bb}.
\end{aligned}$$

This spectral component consists of two Lorentz functions, whose central frequencies are ω_L and linewidths $2\gamma_0^{\pm} = (\Gamma_{1+} + \Gamma_{1-}) \pm \sqrt{(\Gamma_{1+} - \Gamma_{1-})^2 + 4\Gamma_{2+}\Gamma_{2-}}$.

However, the transitions $|a\rangle \to |b\rangle$ and $|b\rangle \to |c\rangle$ lead to the lower-frequency inner sideband, yielding an expression of the form

see equation (27) below

whilst the transitions $|b\rangle \to |a\rangle$ and $|c\rangle \to |b\rangle$ result in the higher-frequency inner sideband,

see equation (28) below.

Since the cavity-induced level shifts are negligibly small, Λ_1 will display a single spectral line located at frequency $\omega_{\rm L} - \Omega_{\rm r}$, and Λ_2 a line at $\omega_{\rm L} + \Omega_{\rm r}$. It is apparent that the inner sidebands are also composed of two Lorentzians with linewidths $2\gamma_1^{\pm} = (\Gamma_{3+} + \Gamma_{3-}) \pm \sqrt{(\Gamma_{3+} - \Gamma_{3-})^2 + 4\Gamma_4^2}$.

The final transitions, $|a\rangle \to |c\rangle$ and $|a\rangle \to |c\rangle$, respectively generate the lower-frequency and higher-frequency spectral lines of the outer sidebands, which are given by

$$\Lambda_3(\omega) = \left[\frac{2\eta^2(1+\epsilon^2)\rho_{aa}}{s + \Gamma_5 + {\rm i}\Omega_5}\right]_{s={\rm i}\omega}, \tag{29}$$

$$\Lambda_4(\omega) = \left[\frac{2\eta^2(1+\epsilon^2)\rho_{cc}}{s + \Gamma_5 - {\rm i}\Omega_5}\right]_{s={\rm i}\omega}. \tag{30}$$

$$\Lambda_1(\omega) = {\rm Re}\left[\frac{4\eta^2[8\eta^2(s + \Gamma_{3+} + {\rm i}\Omega_{3+}) + \epsilon^2\Gamma_4]\rho_{bb} + \frac{\epsilon^2}{2}[(1+\epsilon^2)(s + \Gamma_{3-} + {\rm i}\Omega_{3-}) + 8\eta^2\Gamma_4]\rho_{aa}}{(s + \Gamma_{3+} + {\rm i}\Omega_{3+})(s + \Gamma_{3-} + {\rm i}\Omega_{3-}) - \Gamma_4^2}\right]_{s={\rm i}\omega} \tag{27}$$

$$\Lambda_2(\omega) = {\rm Re}\left[\frac{4\eta^2[8\eta^2(s + \Gamma_{3-} - {\rm i}\Omega_{3-}) + \epsilon^2\Gamma_4]\rho_{bb} + \frac{\epsilon^2}{2}[(1+\epsilon^2)(s + \Gamma_{3+} - {\rm i}\Omega_{3+}) + 8\eta^2\Gamma_4]\rho_{cc}}{(s + \Gamma_{3+} - {\rm i}\Omega_{3+})(s + \Gamma_{3-} - {\rm i}\Omega_{3-}) - \Gamma_4^2}\right]_{s={\rm i}\omega} \tag{28}$$

The spectral lines are centered at frequencies $\omega_{\rm L} \pm 2\Omega_{\rm r}$, respectively, and have width $2\Gamma_5$. In equations (25–30), the ρ_{jj} $(j = a, b, c)$ which appear are the steady-state dressed-state occupation probabilities, given by equations (18).

Equations (26–30) show that when $\delta = 0$, the fluorescence spectrum is symmetric because the decay rates obey $\Gamma_{i+} = \Gamma_{i-}$ $(i = 1, 2, 3)$ and the populations in dressed states satisfy $\rho_{cc} = \rho_{aa}$. Since the Lorentz function $\mathcal{R}(0)$ is absent in the linewidths $2\gamma_0^{\pm}$ of the central peak and present in $2\gamma_1^{\pm}$ and $2\Gamma_5$, the central peak is much narrower than the inner and outer ones when $\delta = 0$. For the case of the atom with two nearly degenerate excited states (for example, $\omega_{21} = 10$ and $\Omega = 100$), equations (27, 28) indicate that the inner sidebands located at $\omega_{\rm L} \pm \Omega_{\rm r}$ are hardly visible because of $\rho_{bb} \approx 0$ and $\epsilon^2 \approx 0$, as illustrated in Figure 2. When $\delta = 2\Omega_{\rm r}$, the transition rates R_{ca} and R_{ac} are enhanced significantly, this means that the outer sidebands are enhanced and narrowed and the central peak is suppressed and broadened. Because $\rho_{aa} > \rho_{cc}$ at $\delta = 2\Omega_{\rm r}$, the lower-frequency sideband is slightly higher than the higher-frequency one.

For the case of $\omega_{21} = 200$ and $\Omega = 300$, by inspection of equation (25) for the decay rates $\Gamma_{i\pm}$ and Γ_5, one finds that when $\delta = 0$, the decay rates $\Gamma_{1\pm}$ and $\Gamma_{2\pm}$ are the same as those in the absence of the stochastic field because of $\Omega_{\rm r} \gg \kappa$, but $\Gamma_{3\pm}$ and Γ_5 are strongly enhanced with the amplitudes $2\eta^2 D$ and $8\eta^2 D$, respectively. So the inner and outer sidebands are significantly broadened and suppressed, whilst the central peak is narrowed and enhanced, as shown in Figure 3a. When the detuning is chosen as $\Omega_{\rm r}$ and $2\Omega_{\rm r}$, γ_0^+ is increased evidently, even larger than $\gamma_1^{\pm}$ and Γ_5, so the central peak can be broader than the inner and the outer sidebands, as illustrated in Figure 3c. Moreover, for $\delta = 2\Omega_{\rm r}$, γ_0^- $(\sim \gamma)$ is much smaller than γ_0^+ $(\sim D/2)$, the central peak consists of one very sharp peak superimposed on a very broad Lorentz profile, which is similar to that in the system of a V-type three-level atom with two nearly parallel dipole moments [21]. The asymmetric feature of the spectrum in Figure 3b can be understood as follows: since $\epsilon^2 = 1/19$, equations (27, 28) show that the peak values of the left and right inner sidebands are mainly dependent on ρ_{bb}/Γ_{3-} and ρ_{bb}/Γ_{3+} respectively, the left inner peak is lower than the right inner one because of $\Gamma_{3-} > \Gamma_{3+}$ for $\delta = \Omega_{\rm r}$. As shown in Figure 1f, $\rho_{aa} > \rho_{cc}$ when $\delta = \Omega_{\rm r}$, so the left outer peak is higher than the right one. But for $\delta = 2\Omega_{\rm r}$, $\Gamma_{3+} \approx \Gamma_{3-}$ and $\rho_{cc} \approx \rho_{aa}$, thus the asymmetric feature almost disappears in Figure 3c. At this moment, ρ_{bb} is much smaller than ρ_{aa} and ρ_{cc} as indicated in Figure 1f, consequently the outer peaks are much higher than the inner ones.

The spectral line narrowing and asymmetric features presented in Figure 4 can be also explained by use of equations (26–30) as well. For example, because of $\rho_{cc} > \rho_{aa}$ when $\delta > 0$ as shown in Figure 1b, the left outer and inner peaks can be higher than the right corresponding ones. However, comparing with Figures 2 and 3, we can see that by adjusting the frequency detuning δ, the spectral line features for $\epsilon^2 \ll 1$ can be controlled more efficiently.

However, when the stochastic field is a complex white noise field, *i.e.*, the bandwidth $\kappa \to \infty$, the properties of resonance fluorescence spectrum differ evidently from those when κ is finite as mentioned in the above. For example, when $\kappa \to \infty$, from equation (26) the central component of the fluorescence spectrum reduces to

$$\Lambda_0(\omega) = 4\eta^2 \mathrm{Re}\left[\frac{2\rho_{aa}}{s + \gamma(1-\epsilon^2)/2 + (1-\epsilon^2/2)D} + \frac{18\epsilon^2\rho_{aa}\rho_{bb}}{s + \gamma(2 - 3\epsilon^2 + 3\epsilon^4)/2 + 3\epsilon^2 D/3}\right]\Bigg|_{s=\mathrm{i}\omega}. \quad (31)$$

The central component is consisted of two Lorentz functions. Only when $\epsilon^2 \to 0$, *i.e.*, the two upper levels are nearly degenerate, one relative narrow peak may be superimposed on a broad Lorentzian profile. Unfortunately, at this moment, the height of this relative narrow peak also tends to zero, which means that the line narrowing becomes hardly visible, which is similar to that when the stochastic field is absent and the two dipole moments are nearly parallel or antiparallel [8,24]. Therefore, using the stochastic field with finite bandwidth provides another way to observe the line narrowing phenomenon in resonance fluorescence.

We note that Narducci *et al.* [25] considered a V-type atomic system in which two excited levels are coupled to the ground state by different laser fields. When one transition is very weakly driven compared to the other, the spectral line arising from fluorescence from the strong transition can be narrowed. The spectral narrowing in such a system was later confirmed experimentally by Gauthier *et al.* [26]. The origin of this phenomenon is different from that pointed out in the above. Here we see, because the stochastic field with finite bandwidth forms a frequency-dependent bath for the V-type three-level atom, "tailoring" this bath through adjusting the frequency detuning δ provides an effective way to control the resonance fluorescenced [27].

5 Conclusions

We have investigated the modification of the steady-state populations and resonance fluorescence of a V-type three-level atom driven by a strong coherent field and a weak stochastic field with a wide bandwidth. A strong dependency of the dressed-state populations on the central frequency of the stochastic field is shown. Population inversion can be reached for appropriate Rabi frequency and frequency detuning δ between the coherent field and the stochastic field. If the level gap ω_{21} and the Rabi frequency Ω obey $\omega_{21} < 2\Omega$, then for $\delta < 0$, $\rho_{aa} < \rho_{cc}$, and for $\delta > 0$, $\rho_{aa} > \rho_{cc}$. When $\omega_{21} > 2\Omega$, the situation is reversed. The resultant fluorescence spectrum is also strongly dependent on the central frequency of the stochastic field. When $\delta = 0$, the spectrum is symmetric, and the central peak is much higher and narrower than the inner and outer peaks. If the coherent part of the driving field is very strong, the central peak can be narrowed to

the natural linewidth. When the central frequency of the stochastic field is tuned to resonance with one of the spectral sidebands, the central peak is suppressed and broadened, whilst the inner and outer ones can be enhanced and narrowed. Because the population distributions in the upper and lower dressed states $|c\rangle$ and $|a\rangle$ are asymmetric and the transition rates are different, the inner sidebands and the outer sidebands become asymmetric.

G.X. Li would like to thank Dr. S.Y. Zhu and Prof. S. Swain for their helpful discussions. This work is partially supported by the National Natural Science Foundation of China, Wahan Chenguang Research Project for Young Person and the Natural Science Foundation of Hubei Province, P.R. China.

References

1. B.R. Mollow, Phys. Rev. **188**, 1969 (1969); F.Y. Wu, R.E. Grove, S. Ezekiel, Phys. Rev. Lett. **35**, 1426 (1976).
2. M. Lewenstein, T.W. Mossberg, R.J. Glauber, Phys. Rev. Lett. **59**, 775 (1987); M. Lewenstein, T.W. Mossberg, Phys. Rev. A **37**, 2048 (1988); P. Zhou, S. Swain, Phys. Rev. A **58**, 1515 (1998); J.S. Peng, G.X. Li, P. Zhou, S. Swain, Phys. Rev. A **62**, 063807 (2001).
3. H. Freedhoff, T. Quang, Phys. Rev. Lett. **72**, 474 (1994); M. Loffler, G.M. Meyer, H. Walther, Phys. Rev. A **55**, 3923 (1997).
4. Y. Zhu, A. Lezama, T.W. Mossberg, M. Lewenstein, Phys. Rev. Lett. **61**, 1946 (1988); A. Lezama, Y. Zhu, S. Morin, T.W. Mossberg, Phys. Rev. A **39**, R2754 (1989).
5. W. Lange, H. Walther, Phys. Rev. A **48**, 4551 (1993); G.S. Agarwal, W. Lange, H. Walther, Phys. Rev. A **48**, 4555 (1993).
6. H.J. Carmichael, A.S. Lane, D.F. Walls, Phys. Rev. Lett. **58**, 2539 (1987); N. Lukenhaus, J.I. Cirac, P. Zoller, Phys. Rev. A **57**, 548 (1998).
7. A.S. Parkins, Phys. Rev. A **42**, 4352, 6873 (1990); G. Yeoman, S.M. Barnett, J. Mod. Opt. **43**, 2037 (1996); M.R. Ferhuson, Z. Ficek, B.J. Dalton, Phys. Rev. A **54**, 2379 (1996); B.J. Dalton, S. Swain, J. Mod. Opt. **46**, 379 (1999).
8. D.A. Cardimona, M. Raymer, C.R. Stroud Jr, J. Phys. B **15**, 65 (1982); P. Zhou, S. Swain, Phys. Rev. Lett. **77**, 3995 (1996); Phys. Rev. A **56**, 3011 (1997).
9. S.Y. Zhu, M.O. Scully, Phys. Rev. Lett. **76**, 388 (1996); H. Huang, S.Y. Zhu, M.S. Zubairy, Phys. Rev. A **54**, 744 (1997); M.O. Scully, S.Y. Zhu, Science **281**, 1973 (1998).
10. J.H. Eberly, Phys. Rev. Lett. **37**, 1387 (1976); G.S. Agarwal, P.A. Lakshmi, Phys. Rev. A **35**, 3152 (1987); H. Ritsch, P. Zoller, J. Cooper, Phys. Rev. A **41**, 2653 (1990); A.H. Toor, M.S. Zubairy, Phys. Rev. A **49**, 449 (1994); A.G. Kofman, Phys. Rev. A **56**, 2280 (1996).
11. A.T. Georges, Phys. Rev. A **21**, 2034 (1980); R.E. Ryan, T.H. Bergeman, Phys. Rev. A **43**, 6142 (1991).
12. G.S. Agarwal, S. Singh, Phys. Rev. A **39**, 2239 (1989); G. Vemurim, R. Roy, G.S. Agarwal, Phys. Rev. A **41**, 2749 (1990); G. Vemuri, K.V. Vasavadia, G.S. Agarwal, Phys. Rev. A **50**, 2599 (1994); P. Zhou, S. Swain, Phys. Rev. A **58**, 4705 (1998).
13. P. Zhou, S. Swain, Phys. Rev. Lett. **82**, 2500 (1999).
14. M. Shapiro, J.W. Hepburn, P. Brumer, Chem. Phys. Lett. **149**, 451 (1988); P. Brumer, M. Shapiro, Ann. Rev. Phys. Chem. **43**, 257 (1992).
15. C. Chen, Y.Y. Yin, D.S. Elliott, Phys. Rev. Lett. **64**, 507 (1990).
16. L. Zhu *et al.*, Phys. Rev. Lett. **79**, 4108 (1997).
17. T. Nakajima, P. Lambropoulos, Phys. Rev. Lett. **70**, 1081 (1993); Phys. Rev. A **50**, 595 (1994); G.X. Li, J.S. Peng, Phys. Lett. A **218**, 49 (1996); J. Mod. Opt. **44**, 505 (1997); D. Petrosyan, P. Lambropoulos, Phys. Rev. Lett. **85**, 1843 (2000).
18. Q. Wu *et al.*, Phys. Rev. A **49**, R1519 (1994); **50**, 1474 (1994); C.C. Yu, J.R. Bochinski, T.M.V. Kordich, T. Mossberg, Z. Ficek, Phys. Rev. A **56**, R4381 (1997).
19. E. Paspalakis, P.L. Knight, Phys. Rev. Lett. **81**, 293 (1999); G.X. Li, K. Allart, D. Lenstra, C. Hooijer, Phys. Lett. A **260**, 253 (1999).
20. U. Lambrecht *et al.*, Phys. Rev. A **57**, R3176 (1998).
21. S.Y. Zhu, M.O. Scully, Phys. Rev. Lett. **76**, 388 (1996).
22. M. Fleischhauer, C. Keitel, M.O. Scully, C. Su, Opt. Commun. **87**, 109 (1992).
23. P. Mestre, M. Sargent III, *Elements of Quantum Optics* (Springer-Verlag, 1990); J.S. Peng, G.X. Li, *Introduction to Modern Quantum Optics* (World Scientific, Sigapore, 1998).
24. C.H. Keitel, Phys. Rev. Lett. **83**, 1307 (1999).
25. L.M. Narducci, M.O. Scully, G.L. Oppo, P. Ru, J.R. Tredicce, Phys. Rev. A **42**, 1630 (1990); C.H. Keitel, L.M. Narducci, M.O. Scully, Appl. Phys. B **60**, s153 (1995).
26. D.J. Gauthier, Y. Zhu, T.W. Mossberg, Phys. Rev. Lett. **66**, 2460 (1991).
27. C.H. Keitel, P.L. Knight, L.M. Narducci, M.O. Scully, Opt. Commun. **118**, 143 (1995).